Hydrol. Earth Syst. Sci. Discuss., 8, 6331–6384, 2011
www.hydrol-earth-syst-sci-discuss.net/8/6331/2011/
doi:10.5194/hessd-8-6331-2011
© Author(s) 2011. CC Attribution 3.0 License.

Hydrology and Earth System Sciences Discussions

This discussion paper is/has been under review for the journal Hydrology and Earth System Sciences (HESS). Please refer to the corresponding final paper in HESS if available.

The effect of downscaling on river runoff modeling: a hydrological case study in the Upper Danube Watershed

T. Marke[1], W. Mauser[2], A. Pfeiffer[3], G. Zängl[4], and D. Jacob[5]

[1]Department of Geography, Karl-Franzens University, Graz, Austria
[2]Department of Geography, Ludwig-Maximilians University, Munich, Germany
[3]Meteorological Institute, Ludwig-Maximilians University, Munich, Germany
[4]Deutscher Wetterdienst, Offenbach, Germany
[5]Max-Planck-Institute for Meteorology, Hamburg, Germany

Received: 13 June 2011 – Accepted: 14 June 2011 – Published: 30 June 2011

Correspondence to: T. Marke (thomas.marke@uni-graz.at)

Published by Copernicus Publications on behalf of the European Geosciences Union.

Abstract

In the current study two regional climate models (MM5 and REMO) driven by different global boundary conditions (ERA reanalysis and the ECHAM5 model) are coupled with the uncalibrated hydrological process model PROMET in order to analyze the impact of global boundary conditions, dynamical regionalization and subsequent statistical downscaling (bilinear interpolation, correction of subgrid-scale variability and combined correction of subgrid-scale variability and bias) on river runoff simulation. The results of 12 coupled model runs set up for the catchment of the Upper Danube over the historical period 1971–2000 indicate that the correction of subgrid-scale variability compared to a bilinear interpolation allows for a more accurate simulation of discharge in case of all model configurations and all discharge criteria considered (mean monthly discharge, mean monthly low-flow discharge and mean monthly peak-flow discharge). Further improvements in the hydrological simulations could be achieved by eliminating the biases (in terms of deviations from observed meteorological conditions) inherent in the driving RCM simulations, regardless of the global boundary conditions or RCM applied. Comparing the hydrological results achievable with MM5 and REMO, the application of bias corrected MM5 simulations turned out to allow for a more accurate simulation of discharge volumes while the variance in simulated discharge was often better reflected in case of REMO forcings. The results achieved with different global boundary conditions are characterized by only minor differences. It is, however, noteworthy that all efficiency criteria in case of bias corrected MM5 simulations indicate better performance under ERA40 boundaries, whereas REMO-driven hydrological simulations better correspond to measured discharge under ECHAM5 boundaries. In spite of all downscaling and bias correction efforts described, the RCM-driven hydrological simulations remain less accurate than those achievable with spatially distributed meteorological observations.

HESSD

8, 6331–6384, 2011

1 Introduction

An increase in atmospheric greenhouse gases has been observed over the last decades that is changing the earth's radiation balance and, as a direct consequence, alters weather patterns around the globe (Houghton et al., 1990). In order to develop regional adaptation and mitigation strategies to these climatic changes and the corresponding impacts on the land surface, decision-makers need detailed information on future climate conditions. Global circulation models (GCMs) are utilized to describe climate relevant processes over decades to centuries at the global scale. However, GCM simulations are computationally limited to coarse spatial resolutions and are therefore unsuitable for climate change impact analysis at the regional scale (Kunstmann et al., 2004). Particularly in areas with complex topography and land use distribution like the Alps, GCMs are not capable of providing temperature and precipitation patterns with sufficient spatial detail (Christensen et al., 2007). Due to the existing limitations in the spatial resolution of GCM simulations, different downscaling techniques are currently applied to provide the climate research community with climate information at higher spatial detail than presently achievable with GCMs. One method that is commonly referred to as statistical downscaling consists in the application of quantitative relations between observed large-scale circulation and small-scale local climate (Wilks, 1995; Wilby et al., 1999; Cubasch, 2001). Another method that is often pursued by nesting regional climate models (RCMs) into GCM simulations is the dynamical downscaling approach (Giorgi and Mearns, 1991; Leung et al., 2004). Driven by the global simulations, RCMs describe atmospheric processes at higher spatial resolution within a spatially limited geographic area. Still, the spatial resolution at which atmospheric processes can be resolved by RCMs is computationally limited to at best 10×10 km at present and does not fully meet the high demands of climate impact models operating at the land surface. Further limitations in the application of RCM data for climate change impact studies carried out with uncalibrated process models result from biases in the RCM simulations in terms of deviations from observation-based datasets (e.g.

HESSD
8, 6331–6384, 2011

biases in simulated temperature and precipitation). Studies by Kotlarski et al. (2005) carried out on a monthly time basis show that biases vary depending on the model used for dynamical regionalization, geographical region and the observation-based meteorological reference data considered. Possible explanations for their origin are manifold and range from regional and local factors such as topography to the influence of maritime and continental air masses (Kotlarski et al., 2005). Jacob et al. (2007) show that the performance of RCMs depends on the global forcing applied to drive the RCMs at the boundaries of the model domain. While reanalysis data can be considered to supply (almost) perfect boundary conditions and are therefore used for model validation, the application of GCM data as global boundaries, which is a prerequisite for climate change investigations, introduces biases in RCM simulations that can be traced back to the global boundaries (Jacob et al., 2007).

In the past many studies have analyzed biases in RCM simulations (e.g. Kotlarski et al., 2006; Jacob et al., 2007; Pfeiffer and Zängl, 2010) or the performance of downscaling techniques, mainly with emphasis on their capabilities in the generation of spatial distributions of daily temperature and precipitation (e.g. Leung et al., 2003; Früh et al., 2006). Further studies exist that directly compare statistically and dynamically downscaled climate model output (e.g. Kidson and Thompson, 1998; Mearns et al., 1999; Murphy, 1999). However, existing studies often consider single combinations of global and regional models making it hard to isolate the effect of boundary conditions on RCM results. Furthermore, there are only few studies that analyze the effect of different downscaling approaches with respect to their implications on the results of impact assessment models. Wilby et al. (2000) use daily precipitation and daily minimum and maximum temperature derived from statistically and dynamically downscaled climate model output (National Center for Atmospheric Research reanalysis) as meteorological input for the Precipitation-Runoff Modeling System (PRMS) (Leavesley and Stannard, 1995) in southwest Colorado. Their results indicate that statistical approaches result in better reproduction of discharge variance, whereas a dynamical downscaling better reproduces total runoff. Wood et al. (2004) evaluate six different downscaling approaches

HESSD
8, 6331–6384, 2011

applied to refine from the GCM scale (T42 resolution) and from the RCM scale (1/2 degree resolution) to the scale of a hydrological model set up for the Columbia River Basin of the US Pacific Northwest region. The hydrological model applied is the Variable Infiltration Capacity (VIC) (Liang et al., 1994) model, a semi-distributed grid-based model, which parameterizes hydrometeorological processes at the land surface-atmosphere interface and operates at a spatial resolution of 1/8 degree and a daily temporal resolution (Wood et al., 2004). These authors, in agreement with Wilby et al. (2000), show that the elimination of biases in the climate simulations significantly improves the results of the hydrological model, e.g. by removing cold biases that affect the simulation of snow processes and in consequence the temporal storage of water in the snow-pack.

The current study was initiated in the framework of the GLOWA-Danube project (www.glowa-danube.de) where RCMs together with a stochastic climate generator are used to supply the model system DANUBIA with the meteorological information required to simulate climate change impacts on the multiple aspects of the water resources in the Upper Danube Watershed (Central Europe). DANUBIA comprises the knowledge of experts from a broad range of natural and social sciences (e.g. meteorology, hydrology, agronomy, tourism and economy) (Mauser and Ludwig, 2002). The model system consists of tightly coupled submodels containing the essential physical and socio-economic process descriptions needed to quantitatively describe the interactions of the different disciplines concerned with water fluxes (Mauser et al., 2002; Ludwig et al., 2003a). GLOWA-Danube strictly follows what has been formulated by Wood et al. (2004) as a de facto minimum standard of any useful downscaling method for hydrological applications: ”the historic (observed) conditions must be reproducible”. From our understanding, this not only applies to the meteorological data used as input for impact models but also for the results of the impact models themselves. The present work investigates the potential and limitations of an application of RCM simulations as input for the hydrological model component in DANUBIA. We present a set of 12 coupled model runs that have been set up for the period 1971–2000 to separately investigate the impact of global boundary conditions, dynamic regionalization (RCMs)

HESSD
8, 6331–6384, 2011

and subsequent statistical downscaling on the results of the physically based, uncalibrated hydrological process model PROMET (Mauser and Bach, 2009). Please note that care has been taken to assure a comparable spatial resolution for the RCMs used in this study to exclude systematic biases induced by different spatial RCM resolutions. With a total number of 7 meteorological input parameters (precipitation, temperature, wind speed, air humidity, incoming shortwave and longwave radiation, surface pressure) at a temporal resolution of 1 h and a spatial resolution of 1 × 1 km, the demands of the hydrological model (HM) on meteorological input data are comparatively high. Analogously to studies by Yarnal et al. (2000) and Wood et al. (2004) the results of the presented model runs are evaluated by comparing the discharge simulated for the outlet of the Upper Danube Watershed at Achleiten to observations. The latter seems an appropriate approach as discharge at Achleiten represents an integrated response (in space and time) of the catchment to the atmospheric forcings applied. The presented results give a comprehensive overview of the dependence of hydrologcial model results on global boundaries, dynamic regionalization (RCMs), statistical downscaling and bias correction and clearly demonstrate the utility of present generation RCMs for hydrological applications. At the same time it becomes evident, that caution has to be taken when interpreting hydrologcial model results without closely considering the setup of the model chain. While the coupled model system has been set up for the period 1971–2000, the evaluation of the hydrological simulations is limited to the time period 1972–2000 in order to provide the hydrological model a spin-up time of one year.

2 Study site

This study has been carried out in the mountainous watershed of the Upper Danube River. Situated in Central Europe, the basin comprises an area of 76 653 km^2 covering parts of Germany, Austria, Switzerland, the Czech Republic and Italy (Fig. 1). Stretching from altitudes of 287 m a.m.s.l. at the outlet in Achleiten (near Passau) up to

HESSD
8, 6331–6384, 2011

4049 m a.m.s.l. at Piz Bernina in the Alpine headwaters, the complex topographic conditions induce strong meteorological gradients. Annual precipitation ranges from 550 to >2000 mm, annual mean temperatures from −4.8 to 9 °C, evapotranspiration from 100 to 700 mm per year and the resulting annual discharge from 150 to 1750 mm per year (Mauser and Bach, 2009). The manifold environmental boundary conditions in the watershed lead to very heterogeneous soils ranging from coarse soils in the Alpine part of the catchment to deeply weathered fine-grained soils in the low-lands of the Danube. Agricultural areas (maize, potatoes, sugar beet and cereals) together with intensively managed meadows cover large parts of the valleys in the lowlands, whereas coniferous and deciduous forests as well as meadows characterize the landscape of the Alpine valleys and moraines (Ludwig et al., 2003b). The gauge in Achleiten, where the Danube leaves the watershed in a west to east direction, plays a major role in the following as the evaluation of all model runs presented in this study is based on comparing simulations and observations at this geographic location.

3 Methods

A hydrometeorological model chain composed of 4 components is used to investigate the effect of downscaling on river runoff simulation (see Fig. 2). Global meteorological data is provided by the ERA40 reanalysis or the ECHAM5 model providing the lateral boundaries for the dynamical downscaling carried out by the RCMs MM5 and REMO. A statistical downscaling is subsequently applied within the model coupler and scaling tool SCALMET to translate from the RCM scale to the scale of the hydrological simulations carried out with the hydrological model PROMET. The different components of the model chain are described in detail in the following paragraphs.

HESSD
8, 6331–6384, 2011

3.1 Global boundary conditions – the ERA40 reanalysis and the ECHAM5 model

Climatological studies require high quality, consistent long-time datasets of observed global meteorology for a variety of tasks, like e.g. identifying trends, driving RCMs or impact models and last but not least the verification of climate models. The ECMWF accordingly compiled all available observational data and processed them using a frozen state-of-the-art global data assimilation system to accomplish an about 40-yr long record of consistent global analyses of atmospheric fields (Uppala et al., 2005). This so-called reanalysis served as an "optimal" observation-based input data set to the RCMs in our study.

For projections into the future, global climate models like ECHAM5 have to be operated running largely free, i.e. without incorporating observational input. ECHAM5 has been developed at the Max Planck Institute for Meteorology and is based on the ECMWF's general circulation model (Roeckner et al., 2003). For validation purposes also simulations of present-day conditions have been performed with ECHAM5 that also serve as RCM input in the context of the present case study. For the typical resolution of T63L31 long-term simulations compare reasonably well concerning storm tracks evaluated on the whole northern hemisphere with ERA40 data (Bengtsson et al., 2006). A closer analysis regarding sensitivity of RCM-simulated precipitation to these two different global sets of input data is given by Pfeiffer and Zängl (2011).

3.2 Dynamical downscaling

3.2.1 The regional climate model MM5

One of the RCMs used in this study is the Pennsylvania State University/National Center for Atmospheric Research Mesoscale Model MM5 (release 3.7.3) (Grell et al., 1994). The model domain spans an area of about 3000 × 3500 km covering most of the European continent at a horizontal resolution of 45 km (see Fig. 3). Thus the model

HESSD
8, 6331–6384, 2011

is able to capture the relevant synoptic-scale phenomena governing the climate in our region of interest. In the vertical, the atmosphere is represented by 29 layers up to a top lid pressure of 100 hPa with an enhanced vertical resolution in the boundary layer to allow for a realistic representation of the complex exchange processes here. The optimal configuration of MM5, i.e. the combination of physics parameterizations used here, with emphasis primarily on precipitation in southern Germany and the northern Alps, has been identified by Pfeiffer and Zängl (2010) on the basis of a contiguous ten-year simulation of the 1990ies driven with ERA40 data. The most important parameterizations and schemes employed are summarized as follows. The explicit mixed-phase moisture scheme by Reisner et al. (1998) and the Kain-Fritsch-2 moist convection scheme (Kain, 2004; Kain and Fritsch, 1990, 1993) are directly involved in the generation of precipitation. Radiation is accounted for by the so-called cloud radiation scheme by Dudhia (1993) allowing for direct interaction of resolved clouds with long- and shortwave radiation. The boundary layer is parameterized following Janjic (1994) based on Mellor-Yamada-type prediction of turbulent kinetic energy. Coupled to the boundary layer is the so-called NOAH-LSM (Chen and Dudhia, 2001a, 2001b), a medium-complexity land-surface/vegetation module providing a realistic annual cycle of lower boundary conditions. This scheme has been slightly modified to correct for some inaccuracies as described by Pfeiffer and Zängl (2010). Moreover, the truly horizontal numerical diffusion scheme implemented by Zängl (2002) turned out to be essential for obtaining realistic precipitation patterns in mountainous areas.

3.2.2 The regional climate model REMO

The regional climate model REMO is based on the Europa-Modell, which constitutes the former regional weather prediction model of the German Weather Service (Majewski, 1991; Jacob et al., 2001). REMO is a hydrostatic atmospheric circulation model based on the primitive equations of atmospheric motion, which are solved in a terrain-following hybrid vertical coordinate system. Atmospheric processes in REMO are described for 27 vertical layers with level intervals increasing from the lower atmospheric

HESSD
8, 6331–6384, 2011

levels to the higher atmosphere. Temporal integration is approached using a leap-frog scheme with semi-implicit correction in combination with an Asselin-Filter. The physical parameterizations used in this study have been adopted with some scale-dependent adjustments from the ECHAM4 model (Roeckner et al., 1996) and can be summarized as follows (MPI, 2010). Soil heat is transferred between five soil layers with zero heat flux at the bottom (10 m). The calculation of turbulent surface fluxes is based on the Monin-Obukhov similarity theory (Louis, 1979), and the coefficients for eddy diffusion are determined as functions of the turbulent kinetic energy. For radiation, a scheme after Morcrette et al. (1986) is applied that has been modified for additional greenhouse gases, the 14.6 µm band of ozone and various types of aerosols. Water content in stratiform clouds is described by a budget equation considering sources and sinks related to phase changes and precipitation formation by coalescence of cloud droplets and gravitational settling of ice crystals (Sundquist, 1978). In contrast to MM5, precipitation is computed diagnostically, neglecting horizontal transports of precipitation. The mass flux convection scheme after Tiedtke (1989) is applied for the description of cumulus convection with modifications after Nordeng (1994). The convective cloud water detrained at the top of cumulus clouds is applied as a source term in the stratiform cloud water equation (Roeckner et al., 1996).

3.3 Statistical downscaling – the coupling and scaling tool SCALMET

SCALMET has been developed in the framework of the GLOWA-Danube project as part of the decision support system DANUBIA. Within DANUBIA, SCALMET performs a synchronized exchange of energy and water fluxes between the models for the land surface and the atmosphere. As the simulation of atmospheric processes in present-generation RCMs is still limited to relatively coarse spatial resolutions ($\geq 10 \times 10$ km), adequate scaling techniques have been implemented in the software interface SCALMET to bridge the gap between the model scales. The scaling methods applied combine direct interpolation methods also found in other state of the art couplers (e.g. the OASIS coupler) (Redler et al., 2010), with both statistical and quasi-physical scaling

HESSD
8, 6331–6384, 2011

techniques in order to facilitate the consideration of subgrid-scale heterogeneities within the scaling process. One of the main technical principles in SCALMET is that the down- and upscaling is carried out at runtime of the coupled model system. Hence, the complexity of the scaling algorithms applied is somehow limited for the sake of computational efficiency.

For the present study, a hierarchy of downscaling approaches with different complexity is applied in order to analyze the implications of the different downscaling techniques on the quality of the hydrological model results. The approaches applied consist of:

i. bilinear interpolation

ii. statistical downscaling with conservation of mass and energy

iii. statistical downscaling with bias correction (no conservation of mass and energy)

The bilinear interpolation approach is the most straightforward remapping algorithm of the three methods listed above. It merely considers the neighborhood of surrounding coarse grid raster elements for the estimation of a fine-grid pixel value and does therefore not account for the subgrid-scale variability of a given meteorological parameter. The bilinear interpolation will be referred to by the abbreviation *bil* in the following.

The statistical downscaling approaches applied have been developed for the downscaling of precipitation in alpine-scale complex terrain by Früh et al. (2006) and have recently been extended upon the application on temperature, wind speed and air humidity by Marke et al. (2011). The downscaling approach refered to as *vari* in the following accounts for the subgrid-scale variability of a meteorological parameter while conserving the mass and energy budget imposed by the RCM simulations at each hourly time step. This is achieved by aggregating grids of monthly observations (1 x 1 km) to the spatial resolution and grid structure of the RCMs. The monthly climatologies used here cover the period 1971–2000 and are generated by the meteorological preprocessor of the hydrological model PROMET as described in more detail later within the description of the HM. A multiplicative correction term is deduced through a relative

HESSD
8, 6331–6384, 2011

comparison of the observation-based meteorology (1 × 1 km) to the bilinearily interpolated, observation-based aggregations (1 × 1 km). As neither averaging nor bilinear interpolation affects the area-integrated value, mass and energy are systematically preserved.

The second statistical downscaling approach refered to in the following as *vari&bias* constrains the downscaled RCM simulations to the mass and energy of the observation-based meteorology and hence corrects biases in the RCM simulations. In this case, the correction term is derived through a relative comparison of the observation-based meteorology (1 × 1 km) and the bilinearily interpolated RCM simulations (1 × 1 km).

As biases in RCM simulations can be expected to affect the accuracy of uncalibrated HMs, the correction of biases seems an appropriate measure to be taken in order to optimize hydrological model performance. This particularly applies to Alpine watersheds, where the seasonal storage of water in the snowpack to a large degree controls the discharge at the outlet of the watersheds. Figure 4 displays the mean temperature and precipitation conditions in the Upper Danube Watershed as simulated by the RCMs REMO and MM5 with different boundary conditions in comparison to an observation-based meteorology. As recently pointed out by various authors, it has to be remarked that deviations from any observational dataset largely depend on the quality of the station recordings (Hagemann et al., 2001; Kotlarski et al., 2005; Pfeiffer and Zängl, 2010). Biases in distributions of meteorological observations can be induced by a higher number of stations in valleys compared to mountain ridges or by a wind-induced underestimation of solid precipitation (Pfeiffer and Zängl, 2010; Sevruk, 1985). When using uncorrected meteorlogical observations to correct RCM simulations as done in our study, all the uncertainties inherent in the observation-based data will compromise the overall results of the model chain. Although such circumstances have to be kept in mind, the hydrological results achieved when using our gridded station recordings as input for the hydrological model prove their high quality as will be shown later in this paper.

HESSD
8, 6331–6384, 2011

As Fig. 3a shows, smallest biases in monthly mean temperature are found for MM5 simulations driven by ERA40 reanalysis data. Here, the largest deviations from the observation-based dataset appear in the winter months with a maximum in January (+0.8 °C), while the simulations are very close to the observations for the rest of the year. Driven by the ECHAM5 model, MM5 overestimates mean temperature from November to April by up to +1.5 °C (December and January), while temperatures are slightly underestimated for the rest of the year with a maximum of underestimation in August (−0.9 °C). REMO driven by ERA40 boundaries overestimates temperatures in the Upper Danube Watershed from April to November with a maximum of +1.7 °C in September, whereas comparatively small deviations from the observation-based dataset characterize the rest of the year. In case of REMO driven by ECHAM5 forcings, highest deviations from the observation-based meteorology are found in April and November with +1.8 °C and +1.2 °C, respectively.

Considering simulated precipitation, the models MM5 and REMO show a slight tendency to overestimate precipitation in the Upper Danube Watershed as displayed in Fig. 3b. In particular the ECHAM5-driven model runs for both RCMs are characterized by a comparatively severe overestimation of precipitation in winter. This overestimation is higher in the MM5 simulations with a maximum of around +50 % in January and February. The tendency to overestimate precipitation in winter can be traced back to the climatological behaviour of the ECHAM5 model, which overestimates the frequency of cyclones in Central Europe and the Mediterranean region. The latter in combination with the Alpine barrier leads to a strong overestimation in orographic precipitation at the northern and southern flanks of the Alps.

The multiplicative downscaling functions of *vari* and *vari&bias* as described above are calculated for the parameters precipitation, wind speed and humidity in advance of the coupled model runs. Within the downscaling process in SCALMET, these functions are used to multiply the bilinearly interpolated RCM simulations at each hourly time step h. In case of RCM-simulated temperature, the multiplicative correction is substituted by an additive correction term to more realistically describe the systematic

HESSD
8, 6331–6384, 2011

temperature decrease with increasing terrain elevation.

The downscaling factors used for the correction of subgrid-scale variability and for a combined correction of subgrid-scale variability and bias in MM5-simulated precipitation (ECHAM5 forcings) are illustrated exemplarily for January in Fig. 4. Compared to the correction of subgrid-scale variability alone, the combined correction of subgrid-scale variability and bias remarkably reduces simulated precipitation for the area of the Upper Danube in January. Largest corrections are carried out in the Alpine foreland, where the overestimation of precipitation in the MM5 simulations as a result of biases in the global boundaries is particularly distinct.

While the statistical downscaling functions of *vari* and *vari&bias* are used for the downscaling of precipitation, wind speed, humidity and temperature as described above, a physically based approach is applied for the downscaling of surface pressure. The method is based on the hydrostatic approximation and ideal gas law and is described in detail by Cosgrove et al. (2003). Due to a lack of recordings, incoming longwave and shortwave radiation is bilinearly interpolated to the resolution of 1 × 1 km in case of all coupled model runs presented in this paper.

In order to analyze the performance of the different downscaling approaches for different global boundary conditions, all downscaling factors described are derived separately for REMO and MM5 simulations with ERA40 reanalysis and ECHAM5 forcings. The total number of coupled model runs analyzed here therefore amounts to 12, setting the basis for an intercomparison of the model results achieved. An overview of the different model runs is given in Fig. 5.

3.4 Hydrological simulations – the mesoscale hydrological model PROMET

The distributed, physically based hydrological model PROMET (Processes of Radiation, Mass and Energy Transfer) (Mauser and Bach, 2009) represents the HM in DANUBIA. The model was initially designed by Mauser and Schädlich (1998) as a SVAT-type evapotranspiration model. It has been applied at different spatial scales ranging from single field scale over to mesoscale watersheds (100 000 km^2) as well as

HESSD
8, 6331–6384, 2011

under a variety of climatological conditions (Bach et al., 2000, 2003a, b; Strasser and Mauser, 2001; Ludwig and Mauser, 2000; Ludwig et al., 2003a).

Following a modular structure, PROMET is composed of the following eight components (see Fig. 6): meteorology, land surface energy and mass balance, vegetation, snow and ice, soil hydraulic and soil temperature (unsaturated zone), ground water (saturated zone), channel flow and man-made hydraulic structures.

The meteorology component provides hourly raster fields of the meteorological parameters temperature, precipitation, wind speed, incoming short- and longwave radiation and air humidity for the process description at the land surface by (i) spatially distributing meteorological recordings taken at 277 weather stations of the German and Austrian Weather Service network or (ii) by reading downscaled simulations from RCMs from a file. While the spatial distribution of station recordings is carried out in a meteorological preprocessor within PROMET, the downscaling of RCM output is performed in the model coupler and scaling tool SCALMET as described in a previous section of this paper.

The spatial distribution of meteorological recordings in PROMET is of particular importance for the course of this study as it not only generates the meteorological input for all model runs not driven by RCM data, but also provides the data basis for the statistical downscaling of RCM simulations. The meteorological station network providing the meteorological data basis in our study is comparatively dense and equally distributed over space. However, the number of stations strongly decreases with increasing terrain elevation leading to a certain underrepresentation of higher altitudes (Marke, 2008). The remapping in the meteorological preprocessor of PROMET is carried out by temporally interpolating the recordings taken at 7 a.m., 2 p.m. and 9 p.m. to hourly values in a first step using a cubic spline interpolation (Van Loan, 1997). The interpolation of precipitation distinguishes between short events (one isolated precipitation recording) and long-term events (repeated recordings). The first precipitation class is temporally interpolated by applying a Gaussian distribution to partition the recorded precipitation amount on the hours before the recording, whereas the class of long-term

HESSD
8, 6331–6384, 2011

events is equally distributed over time. The temporally interpolated time series is then spatially distributed by using an inverse distance weighted interpolation in combination with altitudinal corrections. As precipitation distributions in the Upper Danube are not only controlled by terrain elevation, but are also largely governed by the occurrence of orographic lifting at the northern rim of the Alps as well as luff-lee effects, daily correction factors are used to distribute precipitation beyond the capabilities of the regression approach described above. The latter have been derived from a 10-yr analysis of more than 2000 rainfall gauges in the catchment using the Parameter-elevation Regression on Independent Slope Model (PRISM) (Daly et al., 1994). By multiplying interpolated precipitation by these factors, the complex, small-scale precipitation patterns are considered, still not modifying the total precipitation amounts in the basin.

A number of studies have recently given a detailed demonstration of PROMET's ability in the simulation of water and energy fluxes in the Upper Danube Watershed using spatially distributed observations as meteorological input (e.g. Mauser and Bach, 2009; Marke, 2008; Hank, 2008, and Mürth, 2008, Marke et al., 2011). In the framework of this paper, only a brief overview of the model performance in the uncoupled model setup is given in order to provide a basis for comparison to the results of the 12 coupled model runs presented subsequently. Figure 7 shows the simulated daily discharge at gauge Achleiten for the period 1972–2000 compared to observations.

As the scatter plot in Fig. 7a shows, PROMET is capable of simulating daily variability of water fluxes in the watershed with only small biases. This conclusion is further justified by the efficiency criteria of the coefficient of determination (R^2), as well as the Nash-Sutcliffe model efficiency (NSME) (Nash and Sutcliffe, 1970), with values of 0.81 and 0.75 for R^2 and NSME, respectively. Note that values of NSME range from 1 (perfect fit) to $-\infty$, with a NSME of <0 indicating that the mean value of the observations is a better predictor than the model (Krause et al., 2005).

Figure 7b shows the number of days with discharge above daily discharge Qd as simulated and observed for gauge Achleiten. Again, PROMET is able to reproduce observed discharge conditions at Achleiten with good accuracy. The difference between

HESSD
8, 6331–6384, 2011

the two plotted lines in Fig. 7b indicates only a small tendency to overestimate observed discharge volumes. Finally, a comparison of observations and simulations is given for the mean monthly discharge (MMQ), the mean monthly peak flow discharge (MHQ) and the mean monthly low flow discharge (MNQ) over the period 1972–2000 in Fig. 8. The illustrations reveal largest deviations from the observed discharge volumes in case of all discharge criteria considered in May. As discharge in Achleiten is predominantly governed by snowmelt contributions during this time of the year, the implementation of a sub-pixel approach, which is part of current model developments, might be able to improve model performance in spring due to a more realistic representation of snow-related processes (Mauser and Bach, 2009). Compared to simulated MMQ and MNQ discharge, the simulated course of MHQ is characterized by a higher degree of overestimation. The latter can be explained by the fact that large floods tend to be overestimated as the frequent inundation of riparian areas during peak flow events, as well as the measures taken by reservoir management to reduce extreme floods, have both not been implemented in the HM yet. For more information on PROMET, its validation and parameterization, the reader is referred to Mauser and Bach (2009).

4 Results

The following paragraphs present the results achieved within the 12 coupled model runs carried out with the hydrometeorological model chain as presented in the previous sections of this paper. To clearly distinguish between the model results obtained under the application of different global boundary conditions, the hydrological simulations achieved with ERA40 and ECHAM5 boundaries are discussed separately.

4.1 ERA40 boundary conditions

The results of all ERA-driven model runs are displayed in Figs. 9–12. Figure 9 exhibits that a bilinear interpolation (*bil*) and a correction of sub-grid scale variability without

HESSD
8, 6331–6384, 2011

bias correction (*vari*) result in an overestimation in the number of days with discharge volumes above ~1000 $m^3 s^{-1}$ in case of both RCMs, which becomes rather severe above ~2000 $m^3 s^{-1}$. For MM5 this tendency is less distinct and can be fully resolved by including a correction of biases into the downscaling process, whereas a certain overestimation persists when driving PROMET with REMO simulations, even if the latter are corrected for biases in advance of the coupled model run. Analogously to the observation-driven model run discussed earlier (see Fig. 8), MMQ, MHQ and MNQ tend to be overestimated in case of both RCMs particularly in May (see Figs. 10–12). The degree of overestimation, at least for the coupled model runs without bias correction, with values of up to +54 % (MHQ, MM5 *bil*) and +99 % (MHQ, REMO *bil*) is, however, higher when using the RCMs MM5 and REMO to provide the meteorological input for the HM.

While the correction of subgrid-scale variability only slightly improves the simulation of discharge at gauge Achleiten, the integration of a bias correction into the downscaling process strongly reduces the degree of overestimation in case of both RCMs. The latter is particularly evident for the MM5-driven model runs, where the combined correction of subgrid-scale variability and biases in the RCM data (*vari&bias*) reduces deviations from observed discharge to the same order as for the observation-driven control run. Inaccuracies in simulated MMQ and MNQ primarily consist of a shift of the discharge maximum towards spring, but the general amounts of simulated runoff compare well with the observations. These large improvements in simulated discharge can be attributed to a reduction of water available for runoff in April and May as a result of the correction of biases in MM5-simulated precipitation (see Fig. 3b). Simulated evapotranspiration has been compared for the downscaling approaches *vari* and *vari&bias*, but the resulting differences turned out to be minor in case of both RCMs.

Considering simulated MHQ, the combined correction of subgrid-scale variability and biases in case of both RCMs results in an underestimation of discharge in January and February followed by an overestimation of discharge in April and May. The second half of the year is characterized by very little deviations from observed MHQ in case of the

HESSD
8, 6331–6384, 2011

bias corrected MM5 simulations. Considering the same period of time, the application of bias corrected REMO simulations induces an overestimation of discharge of up to 27 % (October) that cannot be observed in the downscaling approaches of the bilinear interpolation and the correction of subgrid-scale variability only. This overestimation, together with the magnitude of overestimation in the first half of the year lead to a comparatively large overall deviation from observed MHQ in case of REMO *vari&bias*. Table 1 gives a comprehensive overview of different statistical criteria applied to evaluate the results of the different ERA-driven coupled model runs. The illustrated values of R^2 indicate that the consideration of subgrid-scale variability within the downscaling process for all ERA40-driven model runs results in an improved reproduction of the discharge at gauge Achleiten (1972–2000). The integration of a bias correction tends to have a neutral to weakly positive impact on R^2 in case of MM5, but a moderately negative impact in case of REMO. The latter indicates that the variance of discharge at Achleiten can be better reproduced by an application of non bias-corrected ERA-REMO simulations. As R^2 merely considers the covariance and not the difference between the observed and predicted parameter, the Nash-Sutcliffe model efficiency (NSME) and the root mean squared error (RMSE) are consulted to extend the statistical analysis. The values of the NSME and RMSE in Table 1 lead to the conclusion that a combined correction of subgrid-scale variability and bias within the downscaling process further improves the simulation of discharge volumes at gauge Achleiten. This is valid for all RCMs and hydrological criteria considered.

Comparing the values of the statistical criteria for ERA40-MM5- and ERA40-REMO-driven model runs, all criteria suggest that the meteorological data provided by MM5 lead to a more accurate simulation of discharge volumes for all downscaling approaches and all discharge criteria. The higher values of R^2 for simulated MNQ in case of REMO however suggest, that the variance in MNQ discharge is better reflected by the REMO-driven model runs.

At least for the downscaling approach *vari&bias*, the monthly mean temperature, precipitation, humidity and wind speed conditions 1971–2000 are identical for both RCMs

HESSD
8, 6331–6384, 2011

as both models share the same reference data used for the bias correction. Differences in the hydrological model results can therefore only be induced by (i) different temporal dynamics in the RCM data (e.g. rainfall intensities), (ii) by short-term differences in the meteorological fields, (iii) by differences in meteorological parameters that are not affected by the correction of biases (shortwave radiation, longwave radiation, surface pressure) or (iv) by an interaction of different hydrometeorological parameters. To further investigate into this assumption, the rain intensities simulated by MM5 and REMO were analyzed for the Upper Danube Watershed (see Fig. 13). The plots show only minor differences in the precipitation intensities in winter, spring and autumn, whereas comparatively large differences between MM5 and REMO exist in summer. Summer rain intensities derived from REMO simulations seem to be characterized by an underestimation of the frequency of low intensity events, whereas events with high intensities tend to be overestimated in their occurrence. Please note that the hourly observations used as reference data represent temporally disaggregated precipitation recordings. The temporal disaggregation as described in a previous section of this paper might result in smoothing of rain intensities.

The differences in MM5- and REMO-simulated rainfall intensities can probably be traced back to the different convection schemes applied within the two RCMs. Although there are deviations from the observation based intensity distribution in case of MM5 as well, the convection scheme applied in MM5 seems to more realistically reflect the observed conditions in the Upper Danube Watershed. As higher rainfall intensities result in increased runoff generation, this partly explains the better overall performance observed for the coupled ERA40-MM5-driven runs. Further explanations for differences in discharge simulations for the downscaling approach *vari&bias* can be found when taking a closer look at the simulated evapotranspiration. As Fig. 14 shows, evapotranspiration is much higher in the MM5-driven model run resulting in lower water availability for runoff generation. The increased evapotranspiration found in the MM5-driven model run can be attributed to differences in simulated global radiation, which are not eliminated by the bias correction (see Fig. 15). MM5 for all months of the year

HESSD
8, 6331–6384, 2011

simulates significantly higher values of global radiation with a minimum of +15 % in August and a maximum of +56 % in January. While mean monthly temperature, precipitation, wind speed and humidity conditions are identical for both downscaled RCM simulations, additional differences in simulated discharge can arise from differences in the meteorological input at shorter time scales resulting in different hydrological reactions of the land surface. Short-term differences in RCM-simulated temperature and precipitation in winter cause differences in the snow cover distributions simulated by the hydrological model PROMET. The latter might be an explanation for the comparatively large differences in simulated discharge between the MM5- and REMO-driven PROMET run in May (see Figs. 10–12).

4.2 ECHAM5 boundary conditions

The last paragraphs have discussed the HM results achieved with ERA40 reanalysis data as boundary conditions for the RCMs MM5 and REMO. These lateral forcings can be considered as perfect boundaries for the simulation of past meteorological conditions, but are, however, not available for the simulation of climate change scenarios. Scenario simulations require the application of GCMs as lateral boundary conditions that include the radiative forcings defined for different climate change scenarios, like those elaborated by the IPCC (2007). As the climate change signal in meteorological and hydrological simulations can only be investigated by comparing simulations achieved under comparable meteorological boundary conditions, it is necessary to analyze the HM results, which result from the use of GCM data as boundary conditions for MM5 and REMO over the period 1972–2000. The results for all coupled model runs conducted with ECHAM5 boundaries are illustrated in Figs. 16–19. Analyzing the HM results achieved with ECHAM5 boundaries leads to findings very similar to those already discussed for ERA40 boundaries. As Fig. 16 shows, the number of days above daily discharge Qd at gauge Achleiten is severely overestimated in case of both RCMs when ECHAM5 boundaries are applied and no bias correction is carried out. This overestimation appears to be more distinct with ECHAM5 boundaries than

HESSD
8, 6331–6384, 2011

for the ERA40-driven model runs. It can be fully resolved by a correction of biases in MM5 simulations. In case of ECHAM5-driven REMO runs, the combined correction of subgrid-scale variability and biases reduces the overestimation of daily discharge. A certain overestimation remains that is, however, less distinct compared to the results achieved with ERA40 boundaries.

Considering simulated MMQ, MHQ and MNQ, the results of all coupled model runs achieved without bias corrections show an overestimation of discharge in the winter half-year (see Figs. 17–19). The latter is much more pronounced in the MM5-driven simulations, where the overstimation of discharge takes values of +69 %–+92 % (January) depending on the discharge criteria considered. The large amount of overestimation in the non bias-corrected MM5 runs in winter leads to a seasonal course in simulated discharge that strongly differs from the observations, which, in case of all hydrological criteria, are characterized by a clear discharge maximum in summer and a discharge minimum in winter. These deviations from observed conditions result in comparatively low R^2 values of 0.15–0.50 for non bias-corrected MM5 simulations depending on the discharge criteria and downscaling method considered (see Table 2).

In case of REMO, the maximum overestimation is found in April and May, where the values amount to +58 %–+67 % (April) and +56 %–+83 % (May) depending on the discharge criteria considered. Although a tendency to overestimate discharge in the winter half-year can be observed in case of REMO-driven model runs as well, the relative proportions characterized by a maximum in summer and a minimum in winter are better reflected by an application of non bias-corrected REMO simulations leading to higher values of R^2 (0.74–0.95). An explanation for the large degree of overestimation found in all non bias-corrected model runs is given by the distinct overestimation of RCM-simulated precipitation under ECHAM5 forcings (see Fig. 3b). As Figs. 17–19 show, the elimination of biases in the RCM data in addition to the consideration of subgrid-scale variability results in a major improvement of the results of the hydrological model PROMET. In case of both RCMs the overestimation of discharge in winter is strongly reduced and turns into an underestimation for the months of January and

HESSD
8, 6331–6384, 2011

February, which is particularly distinct in case of MHQ. Again, this is due to the reduction of water available for runoff as a result of the correction of simulated precipitation and not due to an increase in monthly evapotranspiration. For MMQ and MNQ, the bias correction leads to a discharge maximum in May. This deviation from the discharge recordings is also observed in the uncoupled model setup and can therefore not be attributed to the RCM simulations applied in the coupled model setup.

Analogously to the analysis of all ERA40-driven model runs, the statistical criteria of the coefficient of determination, the Nash-Sutcliffe model efficiency and the root mean squared error are summarized for all ECHAM5-driven model runs in Table 2. As already observed for ERA boundaries, the combined correction of subgrid-scale variability and biases in the RCM data drastically reduces the biases in simulated discharge for both RCMs and all hydrological criteria considered. Comparing the results for MM5 and REMO simulations, R^2 takes higher values in case of REMO. This again applies to all discharge criteria and downscaling approaches and indicates that the temporal variability of discharge at gauge Achleiten is better represented by the results of ECHAM5-REMO-driven model runs. However, the consideration of the absolute differences between simulated and observed discharge 1972–2000, as done in case of NSME and RSME, suggests that ECHAM5-MM5-driven model runs better reproduce absolute discharge volumes at gauge Achleiten. Similar to the ERA40-driven runs, differences between MM5 and REMO can probably be attributed to different convection schemes (resulting in similar differences in rain intensities for ECHAM5 boundaries as shown in a previous section for ERA forcings, see Fig. 13), differences in simulated global radiation (characterized by much higher values of global radiation in case of MM5) and lower values of evapotranspiration in case of REMO.

HESSD
8, 6331–6384, 2011

5 Conclusions

A hydrometeorological model chain has been presented that has been applied to simulate water and energy fluxes in the catchment of the Upper Danube Watershed at a spatial resolution of 1 × 1 km and on a hourly time basis for the period 1971–2000. To analyze the impact of different global boundaries (ERA40 and ECHAM5) translated to the regional scale by different RCMs (MM5 and REMO) and further refined by downscaling approaches of different complexity (bilinear interpolation, correction of subgrid-scale variability and combined correction of subgrid-scale variability and bias) a total number of 12 model runs have been presented and discussed in this paper. It was shown that the quality of the hydrological simulations largely depends on the global boundaries driving the RCMs, on the dynamical downscaling carried out by the RCMs as well as on the subsequent statistical downscaling applied to further refine the RCM data to the scale of the hydrological application. The authors therefore emphasize the urgent need to carefully consider the setup of any coupled model system before interpreting the model results achieved for past as well as potential future climate conditions.

Compared to a simple bilinear interpolation, the correction of subgrid-scale variability in RCM simulated precipitation, temperature, humidity and wind-speed allows a more accurate simulation of discharge. This tendency has been observed for all model configurations and all discharge criteria considered (MMQ, MHQ and MNQ). However, both downscaling approaches lead to an overestimation of discharge at gauge Achleiten. The latter is observed in case of both RCMs. The overestimation is particularly evident for the time from April to June in case of ERA40 boundaries and is further extended to rest of the year in case of ECHAM5 boundaries. Here, the overestimation of discharge can be traced back to a severe overestimation of precipitation induced by the global boundary conditions. The hydrological results achieved using bias-corrected RCM data as meteorological input for the uncalibrated hydrological model PROMET clearly show that the elimination of biases in RCM simulations represents an inevitable measure

HESSD
8, 6331–6384, 2011

to be taken in order to maximize the overall performance of the hydrometeorological model chain, regardless of the global boundary conditions or RCM applied. Comparing the hydrological simulations resulting from an application of MM5 and REMO, the application of bias corrected MM5 simulations turned out to allow a more accurate simulation of discharge volumes at gauge Achleiten 1972–2000. The variance in simulated discharge, however, was often better reflected in case of REMO-forcings. The latter particularly applies to non bias-corrected ECHAM5-driven model runs, where the seasonal course of discharge at Achleiten is barely reproduced by the HM when MM5 simulations are used as meteorological input.

The correction of biases in the RCM data leads to values of mean monthly precipitation, temperature, air humidity and wind speed for the period 1971-2000 that, in case of both RCMs, are identical to the observation-based data used within the downscaling process. Hence, the causes for differences in discharge simulated on the basis of MM5 and REMO meteorology have to be related to differences in the internal dynamics of the RCMs, to differences in meteorological parameters that are not included in the bias correction, to short-term differences in the meteorological data, or to the interaction of different hydrometeorological parameters. From a general point of view, reasons for differences in RCM simulations can be manifold and extend from different parameterizations over different vertical resolutions to differences in the RCM domains. The analysis of simulated rainfall intensities in the present study reveals an overestimation of high rainfall intensities in the REMO simulations in summer, which, together with the non-linear behavior of runoff generation in the hydrological model, partly explains the increased runoff during this time of the year. Further explanations have been found in the simulated evapotranspiration, which is significantly higher in case of all bias-corrected MM5 runs due to higher values of simulated global radiation. Comparing the results achieved with different global boundary conditions, only minor differences can be identified. It is, however, noteworthy that all efficiency criteria in case of bias corrected MM5 simulations indicate better performance under ERA40 boundaries, whereas REMO-driven HM simulations better correspond to measured

HESSD
8, 6331–6384, 2011

discharge under ECHAM5 boundaries.

Compared to the observation-driven model setup, biases in simulated discharge persist that can not be explained by biases in the mean monthly meteorology but rather by considering the temporal dynamics within the RCM simulations and the interaction of different meteorological parameters (e.g. dependence of relative humidity on temperature and absolute humidity) and hydrological parameters (e.g. dependence of water storage in the snow-pack on temperature and precipitation). Additional research efforts have to be undertaken in order to identify the hydrological implication of spatial resolution associated with the description of atmospheric processes. The latter will be investigated in a follow-up study that compares the HM results achieved with REMO simulations at a horizontal grid resolution of 0.088 degree to the results achieved for a grid size of 0.4 degree as used in the current study.

As the quality of RCM simulations and the amount of bias that has to be corrected largely vary in space and time, the transferability of our results to other geographical regions is somehow limited. Additional studies in subcatchments of the Upper Danube Watershed or other European mesoscale watersheds will help to learn, to which extend the results can be generalized to other regions and will thus help to contribute to a better understanding of the complex hydrometeorological interactions involved.

The downscaling and bias correction methods applied in the current study represent pragmatic approaches that are computationally inexpensive and have proven to be robust for the application in coupled land-atmosphere model systems. As these approaches correct biases on a monthly time basis, it cannot be expected that they apply to the correction of differences between climate model simulations and observed climate on shorter time scales. The uncertainties unfolding from the analysis of the HM results on a monthly time basis are therefore of limited value for hydrological applications that aim at the reproduction of hydrological conditions at much finer temporal scales (e.g. of extreme flood events). Investigating the potential of the presented methods on a higher temporal resolution might therefore be a fruitful area for future research activities.

HESSD
8, 6331–6384, 2011

Acknowledgements. The authors thank the German Ministry for Education and Research (BMBF), the Free State of Bavaria and the Ludwig-Maximilians University Munich (LMU) for funding the GLOWA-Danube project. Thanks also go to the German and Austrian Weather Services for the provision of the station data used in this study as well as to all partners of the GLOWA-Danube project for the fruitful cooperations in the last years.

References

Bach, H., Verhoef, W., and Schneider, K.: Coupling remote sensing observation models and a growth model for improved retrieval of (geo)biophysical information from optical remote sensing data, Remote Sensing for Agriculture, Ecosystems and Hydrology, 4171, 1–11, 2000.

Bach, H., Mauser, W., and Schneider, K.: The use of radiative transfer models for remote sensing data assimilation in crop growth models, in: Precision Agriculture, edited by: Stafford, J. and Werner, A., 35–40, ISBN: 9076998213, 2003a.

Bach, H., Braun, M., Lampart, G., and Mauser, W.: Use of remote sensing for hydrological parameterisation of Alpine catchments, Hydrol. Earth Syst. Sci., 7, 862–876, doi:10.5194/hess-7-862-2003, 2003b.

Barnett, T. P., Adam, J. C., and Lettenmaier, D. P.: Potential impacts of a warming climate on water availability in snow-dominated regions, Nature, 438, 303–309, 2005.

Bengtsson, L., Hodges, K. I., and Roeckner, E.: Storm tracks and climate change, J. Climate, 19, 3518–3543, 2006.

Chen, F. and Dudhia, J.: Coupling an advanced land-surface/hydrology model with the Penn State/NCAR MM5 modeling system. Part I: Model implementation and sensitivity, Mon. Weather Rev., 129, 569–585, 2001a.

Chen, F. and Dudhia, J.: Coupling an advanced land-surface/hydrology model with the Penn State/NCAR MM5 modeling system. Part II: Preliminary model validation, Mon. Weather Rev., 129, 587–604, 2001b.

Christensen, J. H., Carter, T. R., Rummukainen, M., and Amanatidis, G.: Evaluating the performance and utility of regional climate models: the PRUDENCE project, Climatic Change, 81, 1–6, 2007.

Cosgrove, B. A., Lohmann, D., Mitchell, K. E., Houser, P. R., Wood, E. F., Schaake, J. C., Robock, A., Marshall, C., Sheffield, J., Duan, Q., Luo, L., Higgins, R. W., Pinker,

HESSD

8, 6331–6384, 2011

R. T., Tarpley, J. D., and Meng, J.: Real-time and retrospective forcing in the North American Land Data Assimilation System (NLDAS) project, J. Geophys. Res., 108, 1–12, doi:10.1029/2002JD003118, 2003.

Cubasch, U.: Simulations of Regional Climate Change, in: Climate of the 21st century: Changes and Risks, edited by: Lozan, J. L., Graßl, H., and Hupfer, P., Hamburg, Germany, 2001.

Daly, C., Neilson, R. P., and Phillips, D. L.: A statistical–topographic model for mapping climatological precipitation over mountainous terrain, J. Appl. Meteorol., 33, 140–158, 1994.

Dudhia, J.: A nonhydrostatic version of the Penn State/NCAR mesoscale model: Validation tests and simulation of an Atlantic cyclone and cold front, Mon. Weather Rev., 121, 1493–1513, 1993.

Frei, C. and Schär, C.: A precipitation climatology of the Alps from high-resolution rain-gauge observations, Int. J. Climatol., 18, 873–900, 1998.

Früh, B., Schipper, J. W., Pfeiffer, A. and Wirth, V.: A pragmatic approach for downscaling precipitation in alpine-scale complex terrain, Meteorol. Z., 15(6), 631–646, 2006.

Giorgi, F. and Mearns, L. O.: Introduction to special section: Regional climate modelling revisited, J. Geophys. Res., 104, 6335–6352, 1991.

Grell, G. A., Dudhia, J., and Stauffer, D. R.: A description of the fifth-generation Penn State/NCAR mesoscale model (MM5), NCAR/TN-398+STR, National Centre for Atmospheric Research, Boulder, Colorado, USA, 1994.

Hagemann, S., Botzet, M., and Machenhauer, B.: The summer drying problem over southeastern Europe: sensitivity of the limited area model HIRHAM4 to improvements in physical parameterization and resolution, Phys. Chem. Earth, 26, 391–396, 2001.

Hank, T.: A Biophysically Based Coupled Model Approach for the Assessment of Canopy Processes Under Climate Change Conditions, Ph.D. thesis, Department of Geography, Ludwig-Maximilians University, Munich, Germany, 2008.

Houghton, J. T., Jenkins, G. J., and Ephraums, J. J. (Eds.): Climate Change, The IPCC Assessment, Cambridge University Press, 1990.

IPCC: Climate Change 2007: The Physical Science Basis, Contribution of Working Group I to the Fourth Assessment Report of the Intergovernmental Panel on Climate Change, Cambridge University Press, 2007.

Jacob, D.: A note to the simulation of the Annual and Interannual Variability of the Water Budget over the Baltic Sea Drainage Basin, Meteorol. Atmos. Phys., 77(1–4), 61–74, 2001.

HESSD

8, 6331–6384, 2011

Jacob, D., Bärring, L., Christensen, O. B., Christensen, J. H., de Castro, M., Déqué, M., Giorgi, F., Hagemann, S., Hirschi, M., Jones, R., Kjellström, E., Lenderink, G., Rockel, B., Sánchez, E., Schär, C., Seneviratne, S. I., Somot, S., van Ulden, A., and van den Hurk, B.: An intercomparison of regional climate models for Europe: model performance in present-day climate, Climatic Change, 81, 31–52, 2007.

Janjic, Z. I.: The step-mountain eta coordinate model: Further development of the convection, viscous sublayer, and turbulent closure schemes, Mon. Weather Rev., 122, 927–945, 1994.

Jones, P. W.: A User's Guide for SCRIP: A Spherical Coordinate Remapping and Interpolation Package, Version 1.4, Los Alamos National Laboratory, University of California, USA, 1998a.

Jones, P. W.: First- and Second-Order Conservative Remapping Schemes for Grids in Spherical Coordinates, Mon. Weather Rev., 27, 2204–2210, 1998b.

Kain, J. S. and Fritsch, J. M.: A one-dimensional entraining/detraining plume model and its application in convective parameterization, J. Atmos. Sci., 47, 2784–2802, 1990.

Kain, J. S. and Fritsch, J. M.: Convective parameterization for mesoscale models: The Kain-Fritsch scheme. The representation of cumulus convection in numerical models, edited by: Emanuel, K. A. and Raymond, D. J., Meteorological Monograph Series, 24(46), 246 pp., ISBN 1-878220-13-6, 1993.

Kain, J. S.: The Kain-Fritsch convective parameterization: An update, J. Appl. Meteorol., 43, 170–181, 2004.

Kidson, J. W. and Thompson, C. S.: A comparison of statistical and model-based downscaling techniques for estimating local climate variations, J. Climate, 11, 735–753, 1998.

Kotlarski, S., Block, A., Böhm, U., Jacob, D., Keuler, K., Knoche, R., Rechid, D., and Walter, A.: Regional climate model simulations as input for hydrological applications: evaluation of uncertainties, Adv. Geosci., 5, 119–125, 2005, http://www.adv-geosci.net/5/119/2005/.

Krause, P., Boyle, D. P., and Bäse, F.: Comparison of different efficiency criteria for hydrological model assessment, Adv. Geosci., 5, 89–97, 2005, http://www.adv-geosci.net/5/89/2005/.

Kunstmann, H., Schneider, K., Forkel, R., and Knoche, R.: Impact analysis of climate change for an Alpine catchment using high resolution dynamic downscaling of ECHAM4 time slices, Hydrol. Earth Syst. Sci., 8, 1031–1045, doi:10.5194/hess-8-1031-2004, 2004.

Leavesley, G. H. and Stannard, L. G.: The precipitation-runoff modeling system – PRMS, in: Computer Models of Watershed Hydrology, edited by: Singh, V. P., Water Resources Publi-

HESSD
8, 6331–6384, 2011

cations, Highlands Ranch, Colorado, USA, 281–310, 1995.
Leung, L. R., Qian, Y., Bian, X., Washington, W. M., Han, J., and Roads, J. O.: Mid-Century Ensemble Regional Climate Change Scenarios for the Western United States, Climatic Change, 62, 75–113, 2004.
Liang, X., Lettenmaier, D. P., Wood, E. F., and Burges, S. J.: A Simple Hydrologically Based Model of Land Surface Water and Energy Fluxes for General Circulation Models, J. Geophys. Res., 99, 14415–14428, 1994.
Liston, G. E. and Elder, K.: A Meteorological Distribution System for High-Resolution Terrestrial Modeling (MicroMet), J. Hydrometeorol., 7, 217–234, 2006.
Louis, J.-F.: A parametric model of vertical eddy fluxes in the atmosphere, Bound.-Lay. Meteorol., 17, 187–202, 1979.
Ludwig, R. and Mauser, W.: Modelling catchment hydrology within a GIS based SVAT-model framework, Hydrol. Earth Syst. Sci., 4, 239–249, doi:10.5194/hess-4-239-2000, 2000.
Ludwig, R., Mauser, W., Niemeyer, S., Colgan, A., Stolz, R., Escher-Vetter, H., Kuhn, M., Reichstein, M., Tenhunen, J., Kraus, A., Ludwig, M., Barth, M., and Hennicker, R.: Web-based modelling of energy, water and matter fluxes to support decision making in mesoscale catchments – the integrative perspective of GLOWA-Danube, Phys. Chem. Earth, 28, 621–634, 2003a.
Ludwig, R., Probeck, M., and Mauser, W.: Mesoscale water balance modelling in the Upper Danube watershed using sub-scale land cover information derived from NOAA-AVHRR imagery and GIS-techniques, Phys. Chem. Earth, 28, 1351–1364, 2003b.
Majewski, D.: The Europa-Modell of the Deutscher Wetterdienst. ECMWF Seminar on Numerical Methods in Atmospheric Models, 2, 147–191, 1991.
Mauser, W. and Bach, H.: PROMET – Large scale distributed hydrological modelling to study the impact of climate change on the water flows of mountain watersheds, J. Hydrol., 376, 362–377, 2009.
Mauser, W. and Ludwig, R.: GLOWA-DANUBE – a research concept to develop integrative techniques, scenarios and strategies regarding global changes of the water cycle, in: Climatic Change: Implications for the Hydrological Cycle and for Water Management, Advances in Global Change Research, edited by: Beniston, M., Vol. 10, Kluwer Academic Publishers, Dordrecht and Boston, 171–188, 2002.
Mauser, W. and Marke, T.: Climate Change and the Water Resources: Scenarios of low-flow conditions in the Upper Danube Watershed, IAHS Publications, 327, 225–236, 2009.

HESSD
8, 6331–6384, 2011

Marke, T.: Development and Application of a Model Interface to couple Regional Climate Models with Land Surface Models for Climate Change Risk Assessment in the Upper Danube Watershed, Ph.D. thesis, Department of Geography, Ludwig-Maximilians University, Munich, Germany, 2008.

Marke, T., Mauser, W., Pfeiffer, A., and Zängl, G.: A pragmatic approach for the downscaling and bias correction of regional climate simulations: evaluation in hydrological modeling, Geosci. Model Dev. Discuss., 4, 45–63, 2011.

Mearns, L. O., Bogardi, I., Giorgi, F., Matyasovszky, I., and Palecki, M.: Comparison of climate change scenarios generated from regional climate model experiments and statistical downscaling, J. Geophys. Res., 104, 6603–6621, 1999.

Morcrette, J.-J., Smith, L., and Fourquart, Y.: Pressure and temperature dependance of the absorption in longwave radiation parameterizations, Beiträge zur Physik der Atmosphäre, 59, 455–469, 1986.

MPI: http://www.mpimet.mpg.de/wissenschaft/atmosphaere-im-erdsystem/arbeitsgruppen/regionale-klimamodellierung-alt/the-remo-model/remo-model-charcteristics.html, last access: 10 October 2010.

Mürth, M. J.: A Soil Temperature and Energy Balance Model for Integrated Assessment of Global Change Impacts at the regional scale, Ph.D. thesis, Department of Geography, Ludwig-Maximilians University, Munich, Germany, 2008.

Nash, J. E. and Sutcliffe, J. V.: River flow forecasting through conceptual models, a discussion of principles, J. Hydrol., 10, 282–290, 1970.

Nordeng, T. E.: Extended versions of the convective parametrization scheme at ECMWF and their impact on the mean and transient activity of the model in the tropics, ECMWF Research Department, Technical Momorandum No. 206, 1994.

Pfeiffer, A. and Zängl, G.: Validation of climate-mode MM5-simulations for the European Alpine Region, Theor. Appl. Climatol., 101, 93–108, 2010.

Pfeiffer, A. and Zängl, G.: Regional climate simulations for the European Alpine Region – sensitivity of precipitation to large scale flow conditions of driving input data, submitted, 2011.

Redler, R., Valcke, S., and Ritzdorf, H.: OASIS4 – a coupling software for next generation earth system modelling. Geosci. Model Dev., 3, 87–104, 2010.

Reisner, J., Rasmussen, R. M., and Bruintjes, R. T.: Explicit forecasting of supercooled liquid water in winter storms using the MM5 mesoscale model, Q. J. Roy. Meteor. Soc., 124B, 1071-,1107, 1998.

HESSD

8, 6331–6384, 2011

Roeckner, E., Arpe, K., Bentsson, L., Christoph, M., Claussen, M., Dümenil, L., Esch, M., Giorgetta, M., Schlese, U., and Schulzweida, U.: The atmospheric genaral circulation model ECHAM-4: Model description and simulation of present day climate, Max-Planck Institut für Meteorologie, Report No. 218, 1996.

Roeckner, E., Bäuml, G., Bonaventura, L., Brokopf, R., Esch, M., Giorgetta, M., Hagemann, S., Kirchner, I., Kornblueh, L., Manzini, E., Rhodin, A., Schlese, U., Schulzweida, U., and Tompkins, A.: The atmospheric general circulation model ECHAM5. Part I: Model description, Max Planck Institute for Meteorology, Report No. 349, 2003.

Sevruk, B.: Systematischer Niederschlagsmessfehler in der Schweiz, in: Der Niederschlag in der Schweiz, edited by: Sevruk, B., Beiträge zur Geologie der Schweiz – Hydrologie, 31, 65–75, 1985.

Strasser, U. and Mauser, W.: Modelling the spatial and temporal variations of the water balance for the Weser catchment 1965–1994, J. Hydrol., 254(1–4), 199–214, 2001.

Sundquist, H.: A parameterization scheme for non-convective condensation including precipitation including prediction of cloud water content, Q. J. Roy. Meteorol. Soc., 104, 677–690, 1978.

Thornton, P. W., Running, S. W., and White, M. A.: Generating surfaces of daily meteorological variables over large regions of complex terrain, J. Hydrol., 190, 214–251, 1997.

Tiedtke, M.: A comprehensive mass flux scheme for cumulus parameterization in large scale models, Mon. Weather Rev., 117, 1779–1800, 1989.

Uppala, S. M., Kållberg, P. W., Simmons, A. J., Andrae, U., da Costa Bechtold, V., Fiorino, M., Gibson, J. K., Haseler, J., Hernandez, A., Kelly, G. A., Li, X., Onogi, K., Saarinen, S., Sokka, N., Allan, R. P., Andersson, E., Arpe, K., Balmaseda, M. A., Beljaars, A. C. M., van de Berg, L., Bidlot, J., Bormann, N., Caires, S., Chevallier, F., Dethof, A., Dragosavac, M., Fisher, M., Fuentes, M., Hagemann, S., Hólm, E., Hoskins, B. J., Isaksen, V., Janssen, P. A. E. M., Jenne, R., McNally, A. P., Mahfouf, J.-F., Morcrette, J.-J., Rayner, N. A., Saunders, R. W., Simon, P., Sterl, A., Trenberth, K. E., Untch, A., Vasiljevic, D., Viterbo, P., and Woollen, J.: The ERA-40 reanalysis, Q. J. Roy. Meteorol. Soc., 131, 2961–3012, DOI:10.1256/qj.04.176, 2005.

Van Loan, C. F.: Introduction to Scientific Computing, Prentice Hall, 1997.

Wilby, R. L., Hay, L. E., and Leavesley, G. H.: A comparison of downscaled and raw GCM output: Implications for climate change scenarios in the San Juan River Basin, Colorado, J. Hydrol., 225, 67–91, 1999.

HESSD

8, 6331–6384, 2011

Wilby, R. L., Hay, L. E., Gutowski, W. J., Arritt, R. W., Takle, E. S., Pan, Z., Leavesley, G. H., and Clark, M. P.: Hydrological responses to dynamically and statistically downscaled climate model output, Geophys. Res. Lett., 27(8), 1199–1202, 2000.

Wilks, D. S.: Statistical Methods in the Atmospheric Sciences: An Introduction, Academic Press, 1995.

Wood, A. W., Leung, L. R., Sridhar, V., and Lettenmaier, D. P.: Hydrological implications of dynamical and statistical approaches to downscaling climate model outputs, Climatic Change, 62, 189–216, 2004.

Xu, C.-Y.: Climate Change and Hydrologic Models: A Review of Existing Gaps and Recent Research Developments, Water Resour. Manag., 12, 31–50, 1999.

Yarnal, B., Lakhtakia, M. N., Yu, Z., White, R. A., Pollard, D., Miller, D. A., and Lapenta, W. M.: A linked meteorological and hydrological model system: the Susquehanna River Basin Experiment (SRBEX), Global Planet. Change, 25, 149–161, 2000.

Zängl, G.: An improved method for computing horizontal diffusion in a sigma-coordinate model and its application to simulations over mountainous topography, Mon. Weather Rev., 130, 1423–1432, 2002.

HESSD

8, 6331–6384, 2011

Table 1. Performance of the hydrological model PROMET using ERA40-driven MM5 and REMO simulations in combination with different downscaling approaches as meteorological input. The abbreviations represent the coefficient of determination (R^2), the Nash-Sutcliffe model efficiency (NSME) and the root mean squared error (RMSE). All statistical criteria have been calculated on the basis of the mean monthly discharge conditions 1972–2000 ($n = 12$).

RCM (ERA40 boundaries)	Hydrological criterion	Downscaling	R^2	NSME	RMSE ($m^3 s^{-1}$)
MM5	MMQ	*bil*	0.71	−0.59	369.26
		vari	0.84	−0.03	297.25
		vari&bias	0.87	0.75	146.05
	MHQ	*bil*	0.69	−0.97	532.04
		vari	0.83	−0.05	388.82
		vari&bias	0.87	0.69	209.94
	MNQ	*bil*	0.71	−0.14	251.74
		vari	0.84	0.08	225.86
		vari&bias	0.83	0.69	132.00
REMO	MMQ	*bil*	0.84	−2.0	506.98
		vari	0.91	−1.09	423.48
		vari&bias	0.85	0.09	279.46
	MHQ	*bil*	0.67	−3.88	836.02
		vari	0.80	−1.52	601.15
		vari&bias	0.74	−0.33	436.48
	MNQ	*bil*	0.91	−0.39	278.05
		vari	0.95	−0.61	299.15
		vari&bias	0.88	0.30	197.33

HESSD
8, 6331–6384, 2011

Table 2. Performance of the hydrological model PROMET using ECHAM5-driven MM5 and REMO simulations in combination with different downscaling approaches as meteorological input. The abbreviations represent the coefficient of determination (R^2), the Nash-Sutcliffe model efficiency (NSME) and the root mean squared error (RMSE). All statistical criteria have been calculated on the basis of the mean monthly discharge conditions 1972–2000 ($n = 12$).

RCM (ECHAM5 boundaries)	Hydrological criterion	Downscaling	R^2	NSME	RMSE ($m^3 s^{-1}$)
MM5	MMQ	*bil*	0.29	−3.80	641.43
		vari	0.50	−2.87	575.88
		vari&bias	0.86	0.73	152.86
	MHQ	*bil*	0.15	−5.29	949.15
		vari	0.43	−3.25	780.37
		vari&bias	0.80	0.53	259.22
	MNQ	*bil*	0.28	−3.39	493.57
		vari	0.48	−2.96	468.40
		vari&bias	0.83	0.63	142.56
REMO	MMQ	*bil*	0.87	−4.20	667.70
		vari	0.92	−3.45	617.89
		vari&bias	0.86	0.18	264.94
	MHQ	*bil*	0.74	−5.67	977.90
		vari	0.84	−3.69	819.56
		vari&bias	0.81	−0.13	402.39
	MNQ	*bil*	0.90	−2.66	450.21
		vari	0.95	−3.09	476.34
		vari&bias	0.89	0.33	192.12

HESSD
8, 6331–6384, 2011

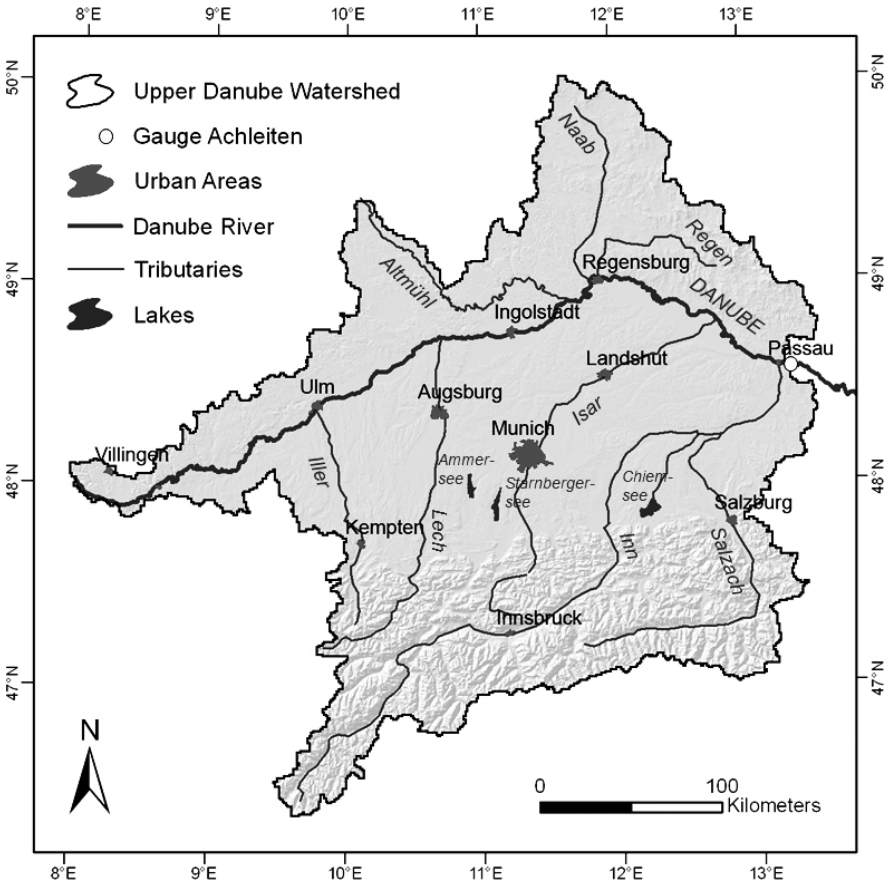

Fig. 1. The Upper Danube Watershed.

HESSD
8, 6331–6384, 2011

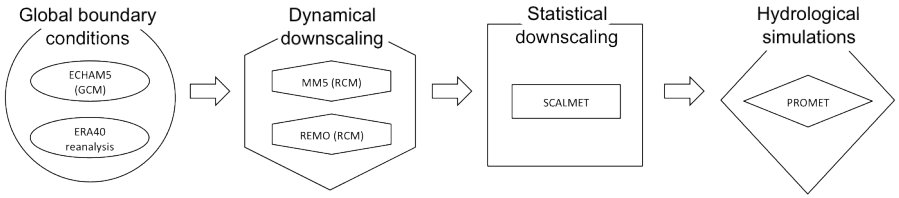

Fig. 2. Schematic overview of the hydrometeorological model chain used in the current study.

HESSD
8, 6331–6384, 2011

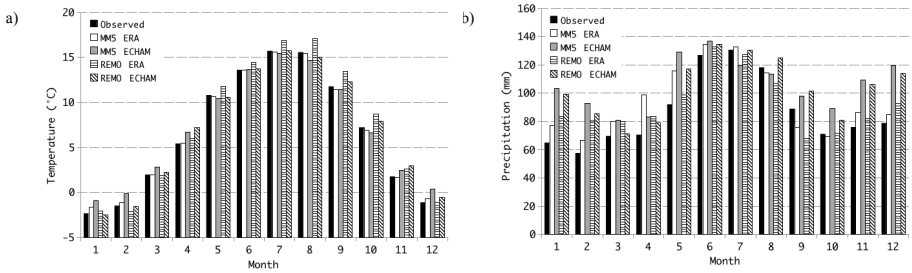

Fig. 3. **(a)** Mean temperature and **(b)** precipitation 1971–2000 as simulated for the Upper Danube Watershed by the RCMs REMO and MM5 compared to observation-based data.

HESSD
8, 6331–6384, 2011

The effect of downscaling on river runoff modeling

T. Marke et al.

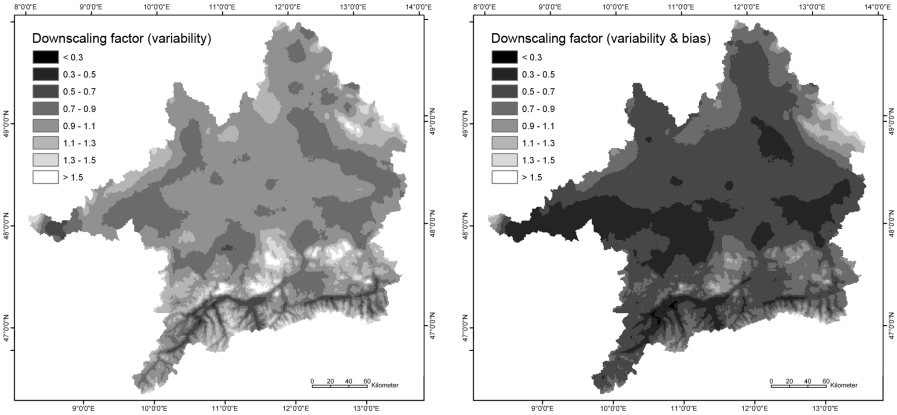

Fig. 4. Downscaling factors for the correction of subgrid-scale variability (1 × 1 km) in MM5 simulated precipitation (45 × 45 km) for January (left) and factors for a combined correction of subgrid-scale variability and bias in MM5 simulated precipitation (ECHAM5 forcings) for January (right).

HESSD
8, 6331–6384, 2011

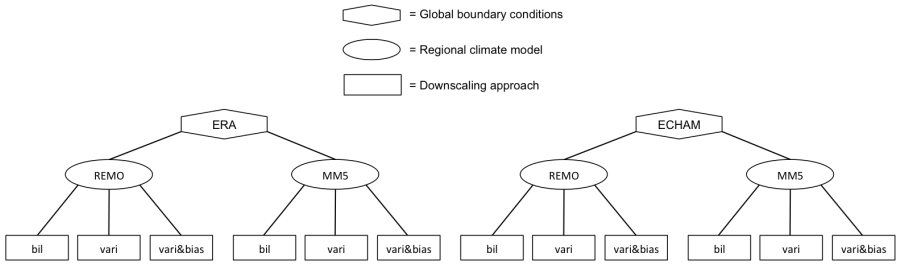

Fig. 5. The coupled model runs analyzed in the framework of this study.

HESSD
8, 6331–6384, 2011

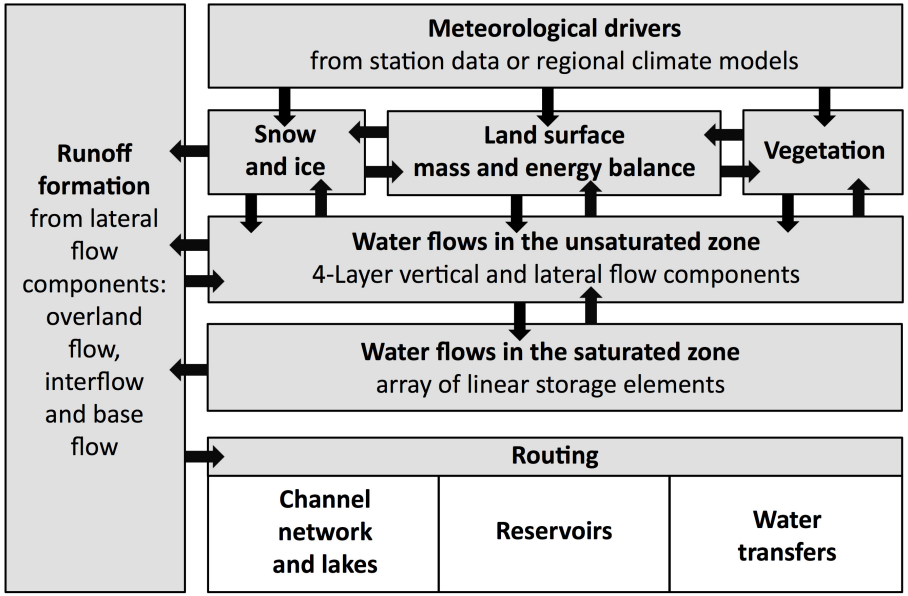

Fig. 6. Schematic diagram of the components of the hydrological model PROMET as used in the current study (boxes) and mass/energy fluxes exchanged between them (arrows).

HESSD
8, 6331–6384, 2011

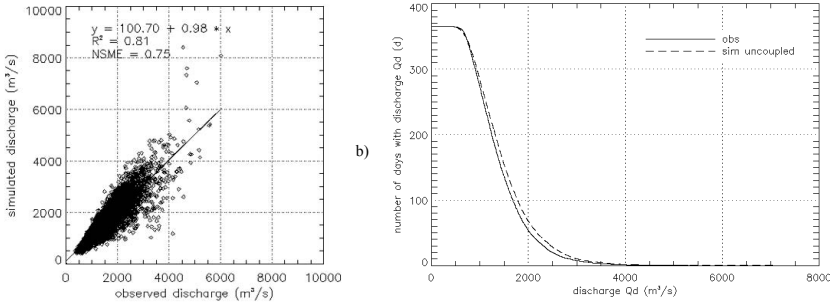

Fig. 7. (a) Daily discharge and **(b)** number of days with discharge above discharge Qd at gauge Achleiten according to observations and uncoupled simulations for the period 1972–2000.

HESSD
8, 6331–6384, 2011

The effect of downscaling on river runoff modeling

T. Marke et al.

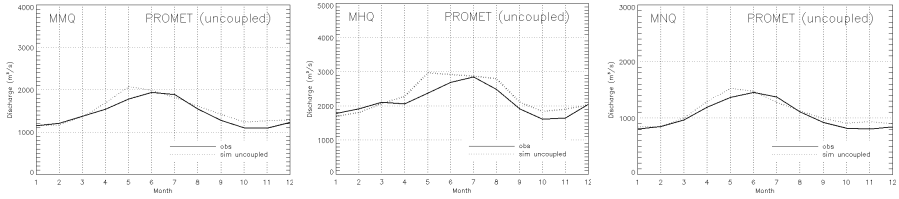

Fig. 8. Mean monthly discharge (MMQ, left), mean monthly peak flow discharge (MHQ, center) and mean monthly low flow discharge (MNQ, right) according to observations and uncoupled simulations for the period 1972–2000.

HESSD
8, 6331–6384, 2011

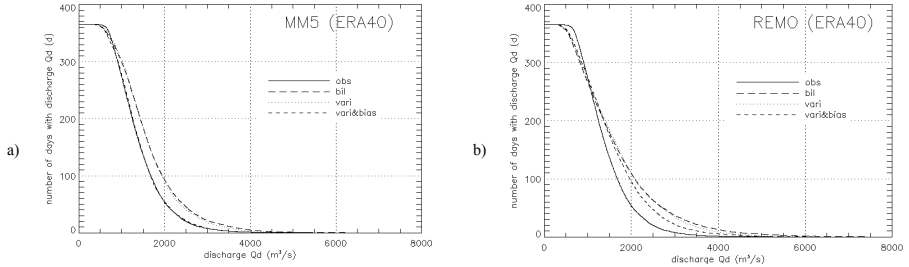

Fig. 9. Comparison of the observed number of days with discharge above discharge Qd at gauge Achleiten to coupled simulations with **(a)** ERA40-MM5 forcings and **(b)** ERA40-REMO forcings for the period 1972–2000.

HESSD
8, 6331–6384, 2011

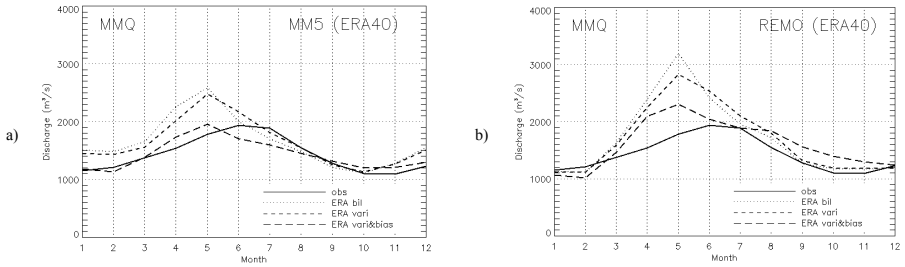

Fig. 10. Comparison of the observed mean monthly discharge (MMQ) at gauge Achleiten to coupled simulations with **(a)** ERA40-MM5 forcings and **(b)** ERA40-REMO forcings for the period 1972–2000.

HESSD
8, 6331–6384, 2011

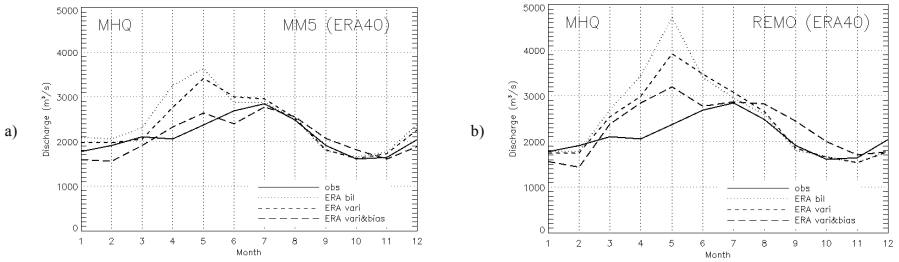

Fig. 11. Comparison of the observed mean monthly peak flow discharge (MHQ) at gauge Achleiten to coupled simulations with **(a)** ERA40-MM5 forcings and **(b)** ERA40-REMO forcings for the period 1972–2000.

HESSD
8, 6331–6384, 2011

The effect of downscaling on river runoff modeling

T. Marke et al.

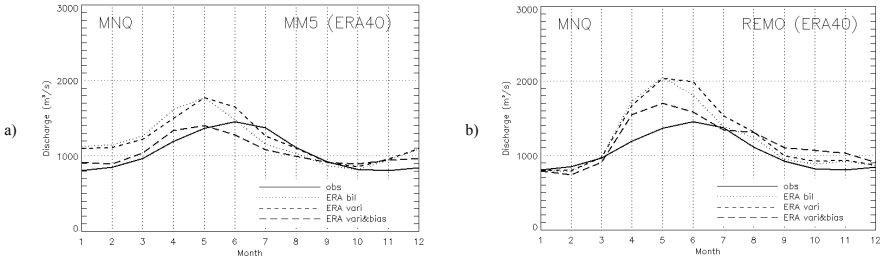

Fig. 12. Comparison of the observed mean monthly low flow discharge (MNQ) at gauge Achleiten to coupled simulations with **(a)** ERA40-MM5 forcings and **(b)** ERA40-REMO forcings for the period 1972–2000.

HESSD
8, 6331–6384, 2011

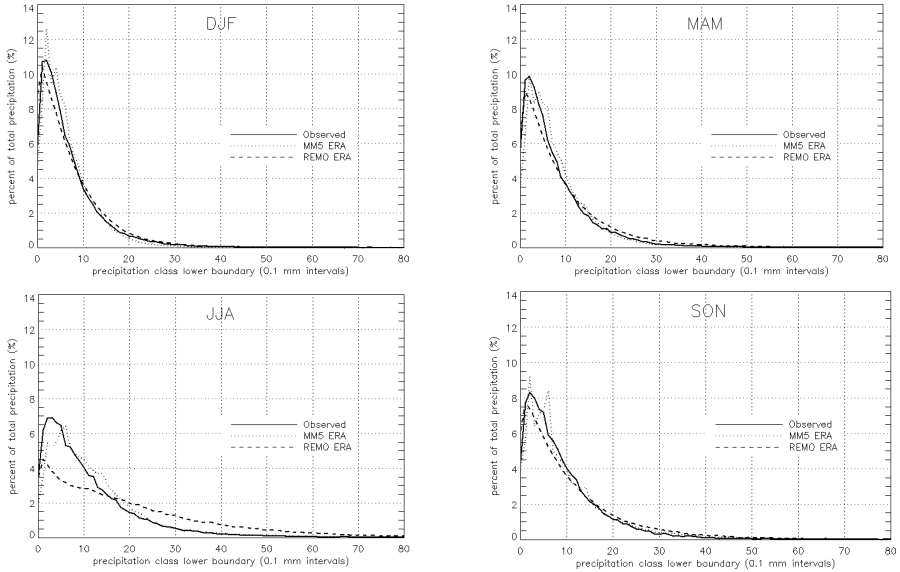

Fig. 13. Mean frequency distribution of hourly precipitation intensities in the Upper Danube Watershed 1972–2000 according to spatially distributed observations (45 × 45 km) and ERA-driven RCM simulations (MM5 45 × 45 km, REMO 50 × 50 km). The observation based precipitation data has been generated by aggregating the calculations of the meteorological preprocessor in PROMET from 1 × 1 km to 45 × 45 km. The abbreviations DJF, MAM, JJA and SON represent the seasons of winter (December, January and February), spring (March, April and May), summer (June, July and August) and autumn (September, October and November).

HESSD
8, 6331–6384, 2011

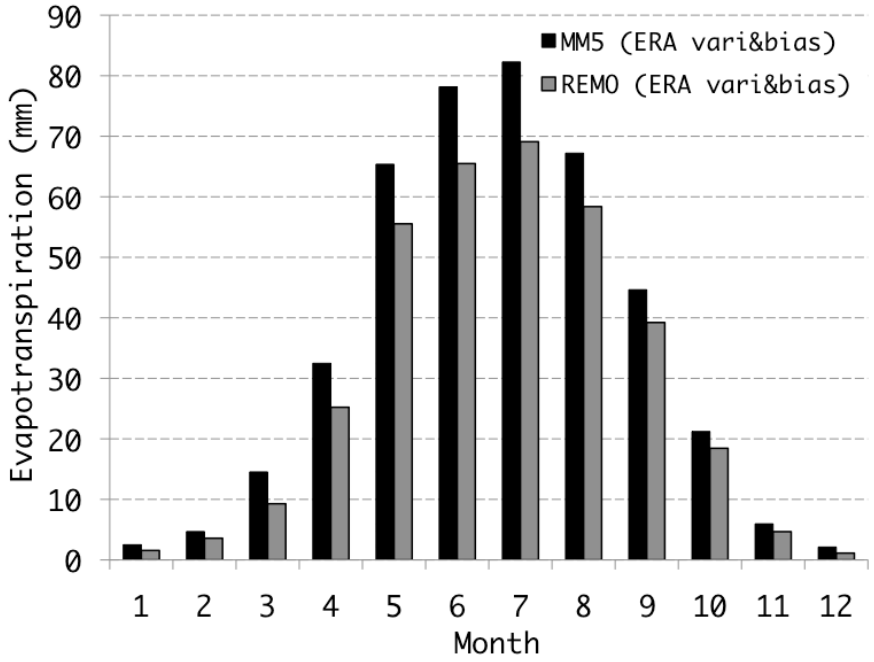

Fig. 14. Monthly mean evapotranspiration simulated on the basis of bias corrected MM5 and REMO simulations (ERA40 boundaries) 1972–2000.

HESSD
8, 6331–6384, 2011

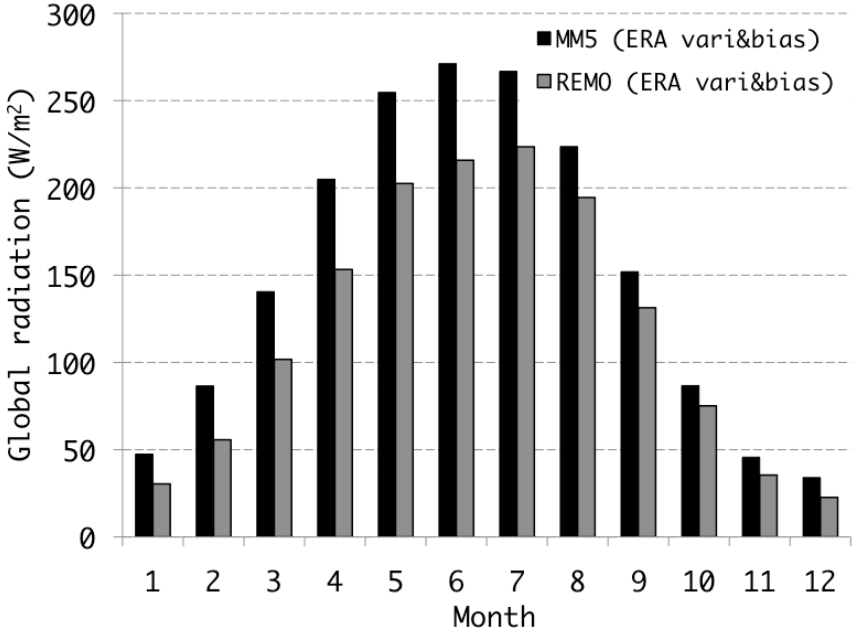

Fig. 15. Monthly mean global radiation as derived from MM5 and REMO simulations (ERA40 boundaries) 1972–2000.

HESSD
8, 6331–6384, 2011

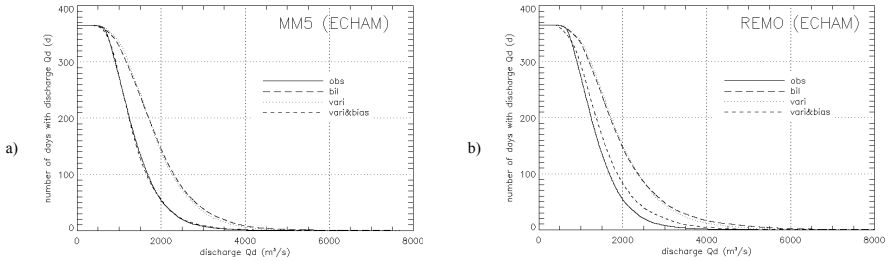

Fig. 16. Comparison of the observed number of days with discharge above discharge Qd at gauge Achleiten to coupled simulations with **(a)** ECHAM5-MM5 forcings and **(b)** ECHAM5-REMO forcings for the period 1972–2000.

HESSD
8, 6331–6384, 2011

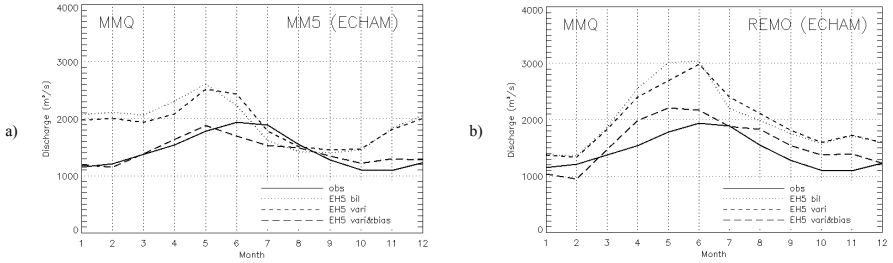

Fig. 17. Comparison of the observed mean monthly discharge (MMQ) at gauge Achleiten to coupled simulations with **(a)** ECHAM5-MM5 forcings and **(b)** ECHAM5-REMO forcings for the period 1972–2000.

HESSD
8, 6331–6384, 2011

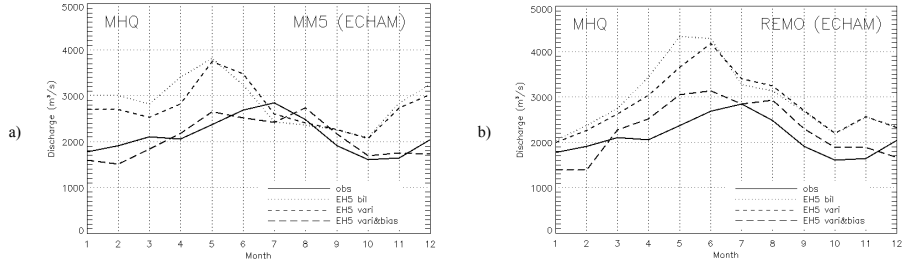

Fig. 18. Comparison of the observed mean monthly peak flow discharge (MHQ) at gauge Achleiten to coupled simulations with **(a)** ECHAM5-MM5 forcings and **(b)** ECHAM5-REMO forcings for the period 1972–2000.

HESSD
8, 6331–6384, 2011

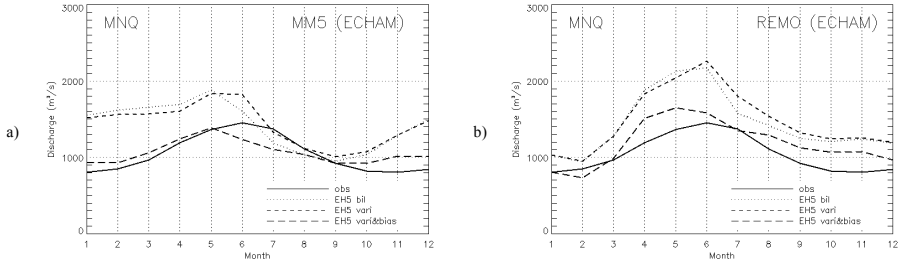

Fig. 19. Comparison of the observed mean monthly low flow discharge (MNQ) at gauge Achleiten to coupled simulations with **(a)** ECHAM5-MM5 forcings and **(b)** ECHAM5-REMO forcings for the period 1972–2000.

HESSD
8, 6331–6384, 2011